Prepared for submission to JINST

Highly-parallelized simulation of a pixelated LArTPC on a GPU

The DUNE Collaboration

A. Abed Abud,[34] B. Abi,[163] R. Acciarri,[67] M. A. Acero,[10] M. R. Adames,[200] G. Adamov,[73] M. Adamowski,[67] D. Adams,[19] M. Adinolfi,[18] C. Adriano,[29] A. Aduszkiewicz,[82] J. Aguilar,[131] Z. Ahmad,[212] J. Ahmed,[215] B. Aimard,[52] F. Akbar,[181] K. Allison,[42] S. Alonso Monsalve,[34] M. Alrashed,[123] C. Alt,[61] A. Alton,[11] R. Alvarez,[38] P. Amedo,[87,86] J. Anderson,[6] D. A. Andrade,[88] C. Andreopoulos,[184,133] M. Andreotti,[95,68] M. P. Andrews,[67] F. Andrianala,[4] S. Andringa,[132] N. Anfimov,[121] W. L. Anicézio Campanelli,[63] A. Ankowski,[190] M. Antoniassi,[200] M. Antonova,[86] A. Antoshkin,[121] S. Antusch,[12] A. Aranda-Fernandez,[41] L. Arellano,[139] L. O. Arnold,[44] M. A. Arroyave,[59] J. Asaadi,[204] A. Ashkenazi,[201] L. Asquith,[198] A. Aurisano,[39] V. Aushev,[129] D. Autiero,[112] M. Ayala-Torres,[40] F. Azfar,[163] A. Back,[92] H. Back,[164] J. J. Back,[215] I. Bagaturia,[73] L. Bagby,[67] N. Balashov,[121] S. Balasubramanian,[67] P. Baldi,[23] W. Baldini,[95] B. Baller,[67] B. Bambah,[83] F. Barao,[132,114] G. Barenboim,[86] P. Barham Alzás,[34] G. J. Barker,[215] W. Barkhouse,[155] C. Barnes,[143] G. Barr,[163] J. Barranco Monarca,[78] A. Barros,[200] N. Barros,[132,62] J. L. Barrow,[140] A. Basharina-Freshville,[210] A. Bashyal,[6] V. Basque,[67] C. Batchelor,[58] J.B.R. Battat,[216] F. Battisti,[163] F. Bay,[3] M. C. Q. Bazetto,[29] J. L. L. Bazo Alba,[176] J. F. Beacom,[161] E. Bechetoille,[112] B. Behera,[43] E. Belchior,[29] L. Bellantoni,[67] G. Bellettini,[104,174] V. Bellini,[94,30] O. Beltramello,[34] N. Benekos,[34] C. Benitez Montiel,[8] D. Benjamin,[19] F. Bento Neves,[132] J. Berger,[43] S. Berkman,[67] P. Bernardini,[98,185] R. M. Berner,[13] A. Bersani,[97] S. Bertolucci,[93,16] M. Betancourt,[67] A. Betancur Rodríguez,[59] A. Bevan,[179] Y. Bezawada,[22] A. T. Bezerra,[63] T. J. Bezerra,[198] J. Bhambure,[195] A. Bhardwaj,[135] V. Bhatnagar,[166] M. Bhattacharjee,[90] M. Bhattacharya,[67] D. Bhattarai,[149] S. Bhuller,[18] B. Bhuyan,[90] S. Biagi,[106] J. Bian,[23] M. Biassoni,[99] K. Biery,[67] B. Bilki,[14,110] M. Bishai,[19] V. Bisignani,[101] A. Bitadze,[139] A. Blake,[130] F. D. Blaszczyk,[67] G. C. Blazey,[156] D. Blend,[110] E. Blucher,[36] J. Boissevain,[134] S. Bolognesi,[33] T. Bolton,[123] L. Bomben,[99,109] M. Bonesini,[99,145] C. Bonilla-Diaz,[31] F. Bonini,[19] A. Booth,[179] F. Boran,[14] S. Bordoni,[34] A. Borkum,[198] N. Bostan,[110] P. Bour,[49] D. Boyden,[156] J. Bracinik,[15] D. Braga,[67] D. Brailsford,[130] A. Branca,[99] A. Brandt,[204] M. Bravo-Moreno,[74] J. Bremer,[34] C. Brew,[184] S. J. Brice,[67] C. Brizzolari,[99,145] C. Bromberg,[144] J. Brooke,[18] A. Bross,[67] G. Brunetti,[99,145] M. Brunetti,[215] N. Buchanan,[43] H. Budd,[181] J. Buergi,[13] G. Caceres V.,[22] I. Cagnoli,[93,16] T. Cai,[222] D. Caiulo,[112] R. Calabrese,[95,68] P. Calafiura,[131] J. Calcutt,[162] M. Calin,[20] L. Calivers,[13] S. Calvez,[43] E. Calvo,[38] A. Caminata,[97] D. Caratelli,[26] D. Carber,[43] J. C. Carceller,[210] G. Carini,[19] B. Carlus,[112] M. F. Carneiro,[19] P. Carniti,[99] I. Caro Terrazas,[43] H. Carranza,[204] N. Carrara,[22] L. Carroll,[123] T. Carroll,[219] A. Carter,[182] J. F. Castaño Forero,[5] A. Castillo,[188] E. Catano-Mur,[218] C. Cattadori,[99] F. Cavalier,[167] G. Cavallaro,[99] F. Cavanna,[67]

S. Centro,[165] G. Cerati,[67] A. Cervelli,[93] A. Cervera Villanueva,[86] K. Chakraborty,[173] M. Chalifour,[34] A. Chappell,[215] E. Chardonnet,[168] N. Charitonidis,[34] A. Chatterjee,[175] S. Chattopadhyay,[212] H. Chen,[19] M. Chen,[23] Y. Chen,[13,190] Z. Chen,[195] Z. Chen-Wishart,[182] Y. Cheon,[209] D. Cherdack,[82] C. Chi,[44] S. Childress,[67] R. Chirco,[88] A. Chiriacescu,[20] N. Chitirasreemadam,[104,174] K. Cho,[126] S. Choate,[156] D. Chokheli,[73] P. S. Chong,[171] B. Chowdhury,[6] A. Christensen,[43] D. Christian,[67] G. Christodoulou,[34] A. Chukanov,[121] M. Chung,[209] E. Church,[164] V. Cicero,[93,16] D. Clapa,[214] P. Clarke,[58] G. Cline,[131] T. E. Coan,[194] A. G. Cocco,[101] J. A. B. Coelho,[168] A. Cohen,[168] J. Collot,[77] E. Conley,[56] J. M. Conrad,[140] M. Convery,[190] S. Copello,[97] P. Cova,[100,169] C. Cox,[182] L. Cremaldi,[149] L. Cremonesi,[179] J. I. Crespo-Anadón,[38] M. Crisler,[67] E. Cristaldo,[100,8] J. Crnkovic,[67] G. Crone,[210] R. Cross,[130] A. Cudd,[42] C. Cuesta,[38] Y. Cui,[25] D. Cussans,[18] J. Dai,[77] O. Dalager,[23] R. Dallavalle,[168] H. da Motta,[32] Z. A. Dar,[218] R. Darby,[198] L. Da Silva Peres,[66] C. David,[222,67] Q. David,[112] G. S. Davies,[149] S. Davini,[97] J. Dawson,[168] K. De,[204] S. De,[1] R. De Aguiar,[29] P. De Almeida,[29] P. Debbins,[110] I. De Bonis,[52] M. P. Decowski,[153,2] A. de Gouvêa,[157] P. C. De Holanda,[29] I. L. De Icaza Astiz,[198] A. Deisting,[138] P. De Jong,[153,2] A. De la Torre,[38] A. Delbart,[33] V. De Leo,[187,105] D. Delepine,[78] M. Delgado,[99,145] A. Dell'Acqua,[34] N. Delmonte,[100,169] P. De Lurgio,[6] J. R. T. de Mello Neto,[66] D. M. DeMuth,[211] S. Dennis,[28] C. Densham,[184] P. Denton,[19] G. W. Deptuch,[19] A. De Roeck,[34] V. De Romeri,[86] G. De Souza,[29] J. P. Detje,[28] R. Devi,[118] R. Dharmapalan,[81] M. Dias,[208] J. S. Díaz,[92] F. Díaz,[176] F. Di Capua,[101,150] A. Di Domenico,[187,105] S. Di Domizio,[97,72] S. Di Falco,[104] L. Di Giulio,[34] P. Ding,[67] L. Di Noto,[97,72] E. Diociaiuti,[96] C. Distefano,[106] R. Diurba,[13] M. Diwan,[19] Z. Djurcic,[6] D. Doering,[190] S. Dolan,[34] F. Dolek,[14] M. J. Dolinski,[55] D. Domenici,[96] L. Domine,[190] S. Donati,[104,174] Y. Donon,[34] S. Doran,[111] D. Douglas,[144] A. Dragone,[190] F. Drielsma,[190] L. Duarte,[208] D. Duchesneau,[52] K. Duffy,[163,67] K. Dugas,[23] P. Dunne,[89] B. Dutta,[202] H. Duyang,[191] O. Dvornikov,[81] D. A. Dwyer,[131] A. S. Dyshkant,[156] M. Eads,[156] A. Earle,[198] D. Edmunds,[144] J. Eisch,[67] L. Emberger,[139,141] P. Englezos,[183] A. Ereditato,[220] T. Erjavec,[22] C. O. Escobar,[67] J. J. Evans,[139] E. Ewart,[92] A. C. Ezeribe,[189] K. Fahey,[67] L. Fajt,[34] A. Falcone,[99,145] M. Fani',[134] C. Farnese,[102] Y. Farzan,[113] D. Fedoseev,[121] J. Felix,[78] Y. Feng,[111] E. Fernandez-Martinez,[137] F. Ferraro,[97,72] L. Fields,[158] P. Filip,[48] A. Filkins,[199] F. Filthaut,[153,180] R. Fine,[134] G. Fiorillo,[101,150] M. Fiorini,[95,68] V. Fischer,[111] R. S. Fitzpatrick,[143] W. Flanagan,[51] B. Fleming,[36,220] R. Flight,[181] S. Fogarty,[43] W. Foreman,[88] J. Fowler,[56] J. Franc,[49] D. Franco,[220] J. Freeman,[67] J. Fried,[19] A. Friedland,[190] S. Fuess,[67] I. K. Furic,[69] K. Furman,[179] A. P. Furmanski,[148] A. Gabrielli,[93,16] A. Gago,[176] H. Gallagher,[207] A. Gallas,[167] A. Gallego-Ros,[38] N. Gallice,[100,146] V. Galymov,[112] E. Gamberini,[34] T. Gamble,[189] F. Ganacim,[200] R. Gandhi,[79] S. Ganguly,[67] F. Gao,[175] S. Gao,[19] D. Garcia-Gamez,[74] M. Á. García-Peris,[86] S. Gardiner,[67] D. Gastler,[17] A. Gauch,[13] J. Gauvreau,[160] P. Gauzzi,[187,105] G. Ge,[44] N. Geffroy,[52] B. Gelli,[29] A. Gendotti,[61] S. Gent,[193] L. Gerlach,[19] Z. Ghorbani-Moghaddam,[97] P. Giammaria,[29] T. Giammaria,[95,68] N. Giangiacomi,[206] D. Gibin,[165,102] I. Gil-Botella,[38] S. Gilligan,[162] A. Gioiosa,[104] S. Giovannella,[96] C. Girerd,[112] A. K. Giri,[91] D. Gnani,[131] O. Gogota,[129] M. Gold,[151] S. Gollapinni,[134] K. Gollwitzer,[67] R. A. Gomes,[64] L. V. Gomez Bermeo,[188] L. S. Gomez Fajardo,[188] F. Gonnella,[15] D. Gonzalez-Diaz,[87] M. Gonzalez-Lopez,[137] M. C. Goodman,[6] O. Goodwin,[139] S. Goswami,[173] C. Gotti,[99] J. Goudeau,[135] E. Goudzovski,[15] C. Grace,[131] R. Gran,[147] E. Granados,[78] P. Granger,[168] C. Grant,[17] D. Gratieri,[71] P. Green,[163]

S. Greenberg,[21,131] L. Greenler,[219] J. Greer,[18] J. Grenard,[34] W. C. Griffith,[198]
F. T. Groetschla,[34] M. Groh,[43] K. Grzelak,[214] W. Gu,[19] V. Guarino,[6] M. Guarise,[95,68]
R. Guenette,[139] E. Guerard,[167] M. Guerzoni,[93] D. Guffanti,[99] A. Guglielmi,[102] B. Guo,[191]
A. Gupta,[190] V. Gupta,[153,2] K. K. Guthikonda,[127] P. Guzowski,[139] M. M. Guzzo,[29] S. Gwon,[37]
C. Ha,[37] K. Haaf,[67] A. Habig,[147] H. Hadavand,[204] A. Hadef,[138] R. Haenni,[13] L. Hagaman,[220]
A. Hahn,[67] J. Haiston,[192] P. Hamacher-Baumann,[163] T. Hamernik,[67] P. Hamilton,[89] J. Han,[175]
J. Hancock,[15] F. Happacher,[96] D. A. Harris,[222,67] J. Hartnell,[198] T. Hartnett,[184] J. Harton,[43]
T. Hasegawa,[125] C. Hasnip,[163] R. Hatcher,[67] K. W. Hatfield,[23] A. Hatzikoutelis,[186] C. Hayes,[92]
K. Hayrapetyan,[179] J. Hays,[179] E. Hazen,[17] M. He,[82] A. Heavey,[67] K. M. Heeger,[220] J. Heise,[197]
S. Henry,[181] M. A. Hernandez Morquecho,[88] K. Herner,[67] V. Hewes,[39] C. Hilgenberg,[148]
T. Hill,[84] S. J. Hillier,[15] A. Himmel,[67] E. Hinkle,[36] L.R. Hirsch,[200] J. Ho,[54] J. Hoff,[67] A. Holin,[184]
T. Holvey,[163] E. Hoppe,[164] G. A. Horton-Smith,[123] M. Hostert,[148] T. Houdy,[167] A. Hourlier,[140]
B. Howard,[67] R. Howell,[181] J. Hoyos Barrios,[142] I. Hristova,[184] M. S. Hronek,[67] J. Huang,[22]
R.G. Huang,[131] Z. Hulcher,[190] G. Iles,[89] N. Ilic,[206] A. M. Iliescu,[93] R. Illingworth,[67]
G. Ingratta,[93,16] A. Ioannisian,[221] B. Irwin,[148] L. Isenhower,[0] M. Ismerio Oliveira,[66] R. Itay,[190]
C.M. Jackson,[164] V. Jain,[1] E. James,[67] W. Jang,[204] B. Jargowsky,[23] F. Jediny,[49] D. Jena,[67]
Y. S. Jeong,[37] C. Jesús-Valls,[85] X. Ji,[19] J. Jiang,[195] L. Jiang,[213] A. Jipa,[20] J. H. Jo,[220]
F. R. Joaquim,[132,114] W. Johnson,[192] B. Jones,[204] R. Jones,[189] N. Jovancevic,[159] M. Judah,[175]
C. K. Jung,[195] T. Junk,[67] Y. Jwa,[44] M. Kabirnezhad,[89] A. Kaboth,[182,184] I. Kadenko,[129]
I. Kakorin,[121] A. Kalitkina,[121] D. Kalra,[44] O. Kamer Koseyan,[110] F. Kamiya,[65] D. M. Kaplan,[88]
G. Karagiorgi,[44] G. Karaman,[110] A. Karcher,[131] Y. Karyotakis,[52] S. Kasai,[128] S. P. Kasetti,[135]
L. Kashur,[43] I. Katsioulas,[15] N. Kazaryan,[221] E. Kearns,[17] P. Keener,[171] K.J. Kelly,[34]
E. Kemp,[29] O. Kemularia,[73] Y. Kermaidic,[167] W. Ketchum,[67] S. H. Kettell,[19] M. Khabibullin,[108]
A. Khotjantsev,[108] A. Khvedelidze,[73] D. Kim,[202] B. King,[67] B. Kirby,[44] M. Kirby,[67] J. Klein,[171]
J. Kleykamp,[149] A. Klustova,[89] T. Kobilarcik,[67] K. Koehler,[219] L. W. Koerner,[82] D. H. Koh,[190]
S. Kohn,[21,131] P. P. Koller,[13] L. Kolupaeva,[121] D. Korablev,[121] M. Kordosky,[218] T. Kosc,[77]
U. Kose,[34] V. A. Kostelecký,[92] K. Kothekar,[18] I. Kotler,[55] V. Kozhukalov,[121] R. Kralik,[198]
L. Kreczko,[18] F. Krennrich,[111] I. Kreslo,[13] W. Kropp,[23] T. Kroupova,[171] M. Kubu,[34]
Y. Kudenko,[108] V. A. Kudryavtsev,[189] S. Kuhlmann,[6] S. Kulagin,[108] J. Kumar,[81] P. Kumar,[189]
P. Kunze,[52] R. Kuravi,[131] N. Kurita,[190] C. Kuruppu,[191] V. Kus,[49] T. Kutter,[135] J. Kvasnicka,[48]
D. Kwak,[209] A. Lambert,[131] B. J. Land,[171] C. E. Lane,[55] K. Lang,[205] T. Langford,[220]
M. Langstaff,[139] F. Lanni,[34] O. Lantwin,[52] J. Larkin,[19] P. Lasorak,[89] D. Last,[171] A. Laundrie,[219]
G. Laurenti,[93] A. Lawrence,[131] P. Laycock,[19] I. Lazanu,[20] M. Lazzaroni,[100,146] T. Le,[207]
S. Leardini,[87] J. Learned,[81] P. LeBrun,[112] T. LeCompte,[190] C. Lee,[67] V. Legin,[129] G. Lehmann
Miotto,[34] R. Lehnert,[92] M. A. Leigui de Oliveira,[65] M. Leitner,[131] L. M. Lepin,[139] S. W. Li,[190]
Y. Li,[19] H. Liao,[123] C. S. Lin,[131] S. Lin,[135] D. Lindebaum,[18] R. A. Lineros,[31] J. Ling,[196]
A. Lister,[219] B. R. Littlejohn,[88] J. Liu,[23] Y. Liu,[36] S. Lockwitz,[67] T. Loew,[131] M. Lokajicek,[48]
I. Lomidze,[73] K. Long,[89] T. Lord,[215] J. M. LoSecco,[158] W. C. Louis,[134] X.-G. Lu,[215]
K.B. Luk,[21,131] B. Lunday,[171] X. Luo,[26] E. Luppi,[95,68] T. Lux,[85] V. P. Luzio,[65] J. Maalmi,[167]
D. MacFarlane,[190] A. A. Machado,[29] P. Machado,[67] C. T. Macias,[92] J. R. Macier,[67]
M. MacMahon,[210] A. Maddalena,[76] A. Madera,[34] P. Madigan,[21,131] S. Magill,[6] K. Mahn,[144]
A. Maio,[132,62] A. Major,[56] K. Majumdar,[133] J. A. Maloney,[50] M. Man,[206] G. Mandrioli,[93]
R. C. Mandujano,[23] J. Maneira,[132,62] L. Manenti,[210] S. Manly,[181] A. Mann,[207]

K. Manolopoulos,[184] M. Manrique Plata,[92] V. N. Manyam,[19] M. Marchan,[67] A. Marchionni,[67] W. Marciano,[19] D. Marfatia,[81] C. Mariani,[213] J. Maricic,[81] F. Marinho,[115] A. D. Marino,[42] T. Markiewicz,[190] D. Marsden,[139] M. Marshak,[148] C. M. Marshall,[181] J. Marshall,[215] J. Marteau,[112] J. Martín-Albo,[86] N. Martinez,[123] D.A. Martinez Caicedo ,[192] F. Martínez López,[179] P. Martínez Miravé,[86] S. Martynenko,[19] V. Mascagna,[99,109] K. Mason,[207] A. Mastbaum,[183] F. Matichard,[131] S. Matsuno,[81] J. Matthews,[135] C. Mauger,[171] N. Mauri,[93,16] K. Mavrokoridis,[133] I. Mawby,[215] R. Mazza,[99] A. Mazzacane,[67] T. McAskill,[216] E. McCluskey,[67] N. McConkey,[210] K. S. McFarland,[181] C. McGrew,[195] A. McNab,[139] A. Mefodiev,[108] P. Mehta,[119] P. Melas,[9] O. Mena,[86] H. Mendez,[177] P. Mendez,[34] D. P. Méndez,[19] A. Menegolli,[103,170] G. Meng,[102] M. D. Messier,[92] W. Metcalf,[135] M. Mewes,[92] H. Meyer,[217] T. Miao,[67] G. Michna,[193] V. Mikola,[210] R. Milincic,[81] G. Miller,[139] W. Miller,[148] J. Mills,[207] O. Mineev,[108] A. Minotti,[99,145] O. G. Miranda,[40] S. Miryala,[19] S. Miscetti,[96] C. S. Mishra,[67] S. R. Mishra,[191] A. Mislivec,[148] M. Mitchell,[135] D. Mladenov,[34] I. Mocioiu,[172] K. Moffat,[57] A. Mogan,[43] N. Moggi,[93,16] R. Mohanta,[83] T. A. Mohayai,[67] N. Mokhov,[67] J. Molina,[8] L. Molina Bueno,[86] E. Montagna,[93,16] A. Montanari,[93] C. Montanari,[103,67,170] D. Montanari,[67] D. Montanino,[98,185] L. M. Montaño Zetina,[40] S. H. Moon,[209] M. Mooney,[43] A. F. Moor,[28] D. Moreno,[5] L. Morescalchi,[104] D. Moretti,[99] C. Morris,[82] C. Mossey,[67] M. Mote,[135] E. Motuk,[210] C. A. Moura,[65] J. Mousseau,[143] G. Mouster,[130] W. Mu,[67] L. Mualem,[27] J. Mueller,[43] M. Muether,[217] F. Muheim,[58] A. Muir,[53] M. Mulhearn,[22] D. Munford,[82] L. J. Munteanu,[34] H. Muramatsu,[148] J. Muraz,[52] M. Murphy,[213] S. Murphy,[61] J. Musser,[92] J. Nachtman,[110] Y. Nagai,[60] S. Nagu,[136] M. Nalbandyan,[221] R. Nandakumar,[184] D. Naples,[175] S. Narita,[116] A. Nath,[90] A. Navrer-Agasson,[139] N. Nayak,[19] M. Nebot-Guinot,[58] K. Negishi,[116] J. K. Nelson,[218] M. Nelson,[110] J. Nesbit,[219] M. Nessi,[67,34] D. Newbold,[184] M. Newcomer,[171] H. Newton,[53] R. Nichol,[210] F. Nicolas-Arnaldos,[74] A. Nikolica,[171] J. Nikolov,[159] E. Niner,[67] K. Nishimura,[81] A. Norman,[67] A. Norrick,[67] P. Novella,[86] J. A. Nowak,[130] M. Oberling,[6] J. P. Ochoa-Ricoux,[23] A. Olivier,[181] A. Olshevskiy,[121] Y. Onel,[110] Y. Onishchuk,[129] J. Ott,[23] L. Pagani,[22] G. Palacio,[59] O. Palamara,[67] S. Palestini,[34] J. M. Paley,[67] M. Pallavicini,[97,72] C. Palomares,[38] S. Pan,[173] W. Panduro Vazquez,[182] E. Pantic,[22] V. Paolone,[175] V. Papadimitriou,[67] R. Papaleo,[106] A. Papanestis,[184] S. Paramesvaran,[18] S. Parke,[67] E. Parozzi,[99,145] S. Parsa,[13] Z. Parsa,[19] S. Parveen,[119] M. Parvu,[20] D. Pasciuto,[104] S. Pascoli,[57,16] L. Pasqualini,[93,16] J. Pasternak,[89] J. Pater,[139] C. Patrick,[58,210] L. Patrizii,[93] R. B. Patterson,[27] S. J. Patton,[131] T. Patzak,[168] A. Paudel,[67] L. Paulucci,[65] Z. Pavlovic,[67] G. Pawloski,[148] D. Payne,[133] V. Pec,[48] S. J. M. Peeters,[198] A. Pena Perez,[190] E. Pennacchio,[112] A. Penzo,[110] O. L. G. Peres,[29] Y. F. Perez Gonzalez,[57] L. Pérez-Molina,[38] C. Pernas,[218] J. Perry,[58] D. Pershey,[56] G. Pessina,[99] G. Petrillo,[190] C. Petta,[94,30] R. Petti,[191] V. Pia,[93,16] F. Piastra,[13] L. Pickering,[182] F. Pietropaolo,[34,102] V. L. Pimentel,[46,29] G. Pinaroli,[19] K. Plows,[163] R. Plunkett,[67] T. Pollman,[153,2] F. Pompa,[86] X. Pons,[34] N. Poonthottathil,[111] F. Poppi,[93,16] S. Pordes,[67] J. Porter,[198] M. Potekhin,[19] R. Potenza,[94,30] B. V. K. S. Potukuchi,[118] J. Pozimski,[89] M. Pozzato,[93,16] S. Prakash,[29] T. Prakash,[131] C. Pratt,[22] M. Prest,[99] F. Psihas,[67] D. Pugnere,[112] X. Qian,[19] J. L. Raaf,[67] V. Radeka,[19] J. Rademacker,[18] R. Radev,[34] B. Radics,[222] A. Rafique,[6] E. Raguzin,[19] M. Rai,[215] M. Rajaoalisoa,[39] I. Rakhno,[67] A. Rakotonandrasana,[4] L. Rakotondravohitra,[4] R. Rameika,[67] M. A. Ramirez Delgado,[171] B. Ramson,[67] A. Rappoldi,[103,170] G. Raselli,[103,170] P. Ratoff,[130] S. Raut,[195] H. Razafinime,[39]

R. F. Razakamiandra,[4] E. M. Rea,[148] J. S. Real,[77] B. Rebel,[219,67] R. Rechenmacher,[67] M. Reggiani-Guzzo,[139] J. Reichenbacher,[192] S. D. Reitzner,[67] H. Rejeb Sfar,[34] A. Renshaw,[82] S. Rescia,[19] F. Resnati,[34] M. Ribas,[200] S. Riboldi,[100] C. Riccio,[195] G. Riccobene,[106] L. C. J. Rice,[175] J. S. Ricol,[77] A. Rigamonti,[34] Y. Rigaut,[61] E. V. Rincón,[59] A. Ritchie-Yates,[182] D. Rivera,[134] R. Rivera,[67] A. Robert,[77] J. L. Rocabado Rocha,[86] L. Rochester,[190] M. Roda,[133] P. Rodrigues,[163] M. J. Rodriguez Alonso,[34] J. Rodriguez Rondon,[192] E. Romeo,[101] S. Rosauro-Alcaraz,[167] P. Rosier,[167] M. Rossella,[103,170] M. Rossi,[34] M. Ross-Lonergan,[134] J. Rout,[119] P. Roy,[217] A. Rubbia,[61] C. Rubbia,[75] G. Ruiz Ferreira,[139] B. Russell,[131] D. Ruterbories,[181] A. Rybnikov,[121] A. Saa-Hernandez,[87] R. Saakyan,[210] S. Sacerdoti,[168] N. Sahu,[91] P. Sala,[100,34] N. Samios,[19] O. Samoylov,[121] M. C. Sanchez,[70] V. Sandberg,[134] D. A. Sanders,[149] D. Sankey,[184] D. Santoro,[100] N. Saoulidou,[9] P. Sapienza,[106] C. Sarasty,[39] I. Sarcevic,[7] I. Sarra,[96] G. Savage,[67] V. Savinov,[175] G. Scanavini,[220] A. Scaramelli,[103] A. Scarff,[189] A. Scarpelli,[19] T. Schefke,[135] H. Schellman,[162,67] S. Schifano,[95,68] P. Schlabach,[67] D. Schmitz,[36] A. W. Schneider,[140] K. Scholberg,[56] A. Schukraft,[67] E. Segreto,[29] A. Selyunin,[121] C. R. Senise,[208] J. Sensenig,[171] D. Sgalaberna,[61] M. H. Shaevitz,[44] S. Shafaq,[119] F. Shaker,[222] M. Shamma,[25] P. Shanahan,[67] R. Sharankova,[207] H. R. Sharma,[118] R. Sharma,[19] R. Kumar,[178] K. Shaw,[198] T. Shaw,[67] K. Shchablo,[112] C. Shepherd-Themistocleous,[184] A. Sheshukov,[121] W. Shi,[195] S. Shin,[120] I. Shoemaker,[213] D. Shooltz,[144] R. Shrock,[195] J. Silber,[131] L. Simard,[167] J. Sinclair,[190] G. Sinev,[192] Jaydip Singh,[136] J. Singh,[136] L. Singh,[47] P. Singh,[179] V. Singh,[47] S. Singh Chauhan,[166] R. Sipos,[34] G. Sirri,[93] A. Sitraka,[192] K. Siyeon,[37] K. Skarpaas,[190] E. Smith,[92] P. Smith,[92] J. Smolik,[49] M. Smy,[23] E.L. Snider,[67] P. Snopok,[88] D. Snowden-Ifft,[160] M. Soares Nunes,[199] H. Sobel,[23] M. Soderberg,[199] S. Sokolov,[121] C. J. Solano Salinas,[107] S. Söldner-Rembold,[139] S.R. Soleti*,[131] N. Solomey,[217] V. Solovov,[132] W. E. Sondheim,[134] M. Sorel,[86] A. Sotnikov,[121] J. Soto-Oton,[38] A. Sousa,[39] K. Soustruznik,[35] F. Spagliardi,[163] M. Spanu,[99,145] J. Spitz,[143] N. J. C. Spooner,[189] K. Spurgeon,[199] D. Stalder,[8] M. Stancari,[67] L. Stanco,[102,165] J. Steenis,[22] R. Stein,[18] H. M. Steiner,[131] A. F. Steklain Lisbôa,[200] A. Stepanova,[121] J. Stewart,[19] B. Stillwell,[36] J. Stock,[192] F. Stocker,[34] T. Stokes,[135] M. Strait,[148] T. Strauss,[67] L. Strigari,[202] A. Stuart,[41] J. G. Suarez,[59] J. Subash,[15] A. Surdo,[98] V. Susic,[12] L. Suter,[67] C. M. Sutera,[94,30] K. Sutton,[27] Y. Suvorov,[101,150] R. Svoboda,[22] S. K. Swain,[154] B. Szczerbinska,[203] A. M. Szelc,[58] A. Taffara,[104] N. Talukdar,[191] J. Tamara,[5] H. A. Tanaka,[190] S. Tang,[19] N. Taniuchi,[28] B. Tapia Oregui,[205] A. Tapper,[89] S. Tariq,[67] E. Tarpara,[19] N. Tata,[80] E. Tatar,[84] R. Tayloe,[92] A. M. Teklu,[195] P. Tennessen,[131,3] M. Tenti,[93] K. Terao,[190] F. Terranova,[99,145] G. Testera,[97] T. Thakore,[39] A. Thea,[184] A. Thompson,[202] C. Thorn,[19] S. C. Timm,[67] V. Tishchenko,[19] N. Todorović,[159] L. Tomassetti,[95,68] A. Tonazzo,[168] D. Torbunov,[19] M. Torti,[99,145] M. Tortola,[86] F. Tortorici,[94,30] N. Tosi,[93] D. Totani,[26] M. Toups,[67] C. Touramanis,[133] R. Travaglini,[93] J. Trevor,[27] S. Trilov,[18] W. H. Trzaska,[122] Y. Tsai,[23] Y.-T. Tsai,[190] Z. Tsamalaidze,[73] K. V. Tsang,[190] N. Tsverava,[73] S. Z. Tu,[117] S. Tufanli,[34] C. Tull,[131] J. Turner,[57] M. Tuzi,[86] J. Tyler,[123] E. Tyley,[189] M. Tzanov,[135] L. Uboldi,[34] M. A. Uchida,[28] J. Urheim,[92] T. Usher,[190] H. Utaegbulam,[199] S. Uzunyan,[156] M. R. Vagins,[124,23] P. Vahle,[218] S. Valder,[198] G. A. Valdiviesso,[63] E. Valencia,[78] R. Valentim,[208] Z. Vallari,[27]

*Corresponding author.

E. Vallazza,[99] **J. W. F. Valle,**[86] **S. Vallecorsa,**[34] **R. Van Berg,**[171] **R. G. Van de Water,**[134] **D. Vanegas Forero,**[142] **D. Vannerom,**[140] **F. Varanini,**[102] **D. Vargas Oliva,**[206] **G. Varner,**[81] **S. Vasina,**[121] **N. Vaughan,**[162] **K. Vaziri,**[67] **J. Vega,**[45] **S. Ventura,**[102] **A. Verdugo,**[38] **S. Vergani,**[28] **M. A. Vermeulen,**[153] **M. Verzocchi,**[67] **M. Vicenzi,**[97,72] **H. Vieira de Souza,**[168] **C. Vignoli,**[76] **C. Vilela,**[34] **B. Viren,**[19] **A. Vizcaya-Hernandez,**[43] **T. Vrba,**[49] **Q. Vuong,**[181] **T. Wachala,**[152] **A. V. Waldron,**[179] **M. Wallbank,**[39] **T. Walton,**[67] **H. Wang,**[24] **J. Wang,**[192] **L. Wang,**[131] **M.H.L.S. Wang,**[67] **X. Wang,**[67] **Y. Wang,**[24] **Y. Wang,**[195] **K. Warburton,**[111] **D. Warner,**[43] **M.O. Wascko,**[89] **D. Waters,**[210] **A. Watson,**[15] **K. Wawrowska,**[184,198] **P. Weatherly,**[55] **A. Weber,**[138,67] **M. Weber,**[13] **H. Wei,**[135] **A. Weinstein,**[111] **D. Wenman,**[219] **M. Wetstein,**[111] **J. Whilhelmi,**[220] **A. White,**[204] **A. White,**[220] **L. H. Whitehead,**[28] **D. Whittington,**[199] **M. J. Wilking,**[195] **A. Wilkinson,**[210] **C. Wilkinson,**[131] **Z. Williams,**[204] **F. Wilson,**[184] **R. J. Wilson,**[43] **W. Wisniewski,**[190] **J. Wolcott,**[207] **J. Wolfs,**[181] **T. Wongjirad,**[207] **A. Wood,**[82] **K. Wood,**[131] **E. Worcester,**[19] **M. Worcester,**[19] **M. Wospakrik,**[67] **K. Wresilo,**[28] **C. Wret,**[181] **S. Wu,**[148] **W. Wu,**[67] **W. Wu,**[23] **M. Wurm,**[138] **J. Wyenberg,**[54] **Y. Xiao,**[23] **I. Xiotidis,**[89] **B. Yaeggy,**[39] **N. Yahlali,**[86] **E. Yandel,**[26] **G. Yang,**[195] **K. Yang,**[163] **T. Yang,**[67] **A. Yankelevich,**[23] **N. Yershov,**[108] **K. Yonehara,**[67] **Y. S. Yoon,**[37] **T. Young,**[155] **B. Yu,**[19] **H. Yu,**[19] **H. Yu,**[196] **J. Yu,**[204] **Y. Yu,**[88] **W. Yuan,**[58] **R. Zaki,**[222] **J. Zalesak,**[48] **L. Zambelli,**[52] **B. Zamorano,**[74] **A. Zani,**[100] **L. Zazueta,**[218] **G. P. Zeller,**[67] **J. Zennamo,**[67] **K. Zeug,**[219] **C. Zhang,**[19] **S. Zhang,**[92] **Y. Zhang,**[175] **M. Zhao,**[19] **E. Zhivun,**[19] **E. D. Zimmerman,**[42] **S. Zucchelli,**[93,16] **J. Zuklin,**[48] **V. Zutshi**[156] **and R. Zwaska**[67]

[0]*Abilene Christian University, Abilene, TX 79601, USA*
[1]*University of Albany, SUNY, Albany, NY 12222, USA*
[2]*University of Amsterdam, NL-1098 XG Amsterdam, The Netherlands*
[3]*Antalya Bilim University, 07190 Döşemealtı/Antalya, Turkey*
[4]*University of Antananarivo, Antananarivo 101, Madagascar*
[5]*Universidad Antonio Nariño, Bogotá, Colombia*
[6]*Argonne National Laboratory, Argonne, IL 60439, USA*
[7]*University of Arizona, Tucson, AZ 85721, USA*
[8]*Universidad Nacional de Asunción, San Lorenzo, Paraguay*
[9]*University of Athens, Zografou GR 157 84, Greece*
[10]*Universidad del Atlántico, Barranquilla, Atlántico, Colombia*
[11]*Augustana University, Sioux Falls, SD 57197, USA*
[12]*University of Basel, CH-4056 Basel, Switzerland*
[13]*University of Bern, CH-3012 Bern, Switzerland*
[14]*Beykent University, Istanbul, Turkey*
[15]*University of Birmingham, Birmingham B15 2TT, United Kingdom*
[16]*Università del Bologna, 40127 Bologna, Italy*
[17]*Boston University, Boston, MA 02215, USA*
[18]*University of Bristol, Bristol BS8 1TL, United Kingdom*
[19]*Brookhaven National Laboratory, Upton, NY 11973, USA*
[20]*University of Bucharest, Bucharest, Romania*
[21]*University of California Berkeley, Berkeley, CA 94720, USA*
[22]*University of California Davis, Davis, CA 95616, USA*
[23]*University of California Irvine, Irvine, CA 92697, USA*

[24]*University of California Los Angeles, Los Angeles, CA 90095, USA*
[25]*University of California Riverside, Riverside CA 92521, USA*
[26]*University of California Santa Barbara, Santa Barbara, California 93106 USA*
[27]*California Institute of Technology, Pasadena, CA 91125, USA*
[28]*University of Cambridge, Cambridge CB3 0HE, United Kingdom*
[29]*Universidade Estadual de Campinas, Campinas - SP, 13083-970, Brazil*
[30]*Università di Catania, 2 - 95131 Catania, Italy*
[31]*Universidad Católica del Norte, Antofagasta, Chile*
[32]*Centro Brasileiro de Pesquisas Físicas, Rio de Janeiro, RJ 22290-180, Brazil*
[33]*IRFU, CEA, Université Paris-Saclay, F-91191 Gif-sur-Yvette, France*
[34]*CERN, The European Organization for Nuclear Research, 1211 Meyrin, Switzerland*
[35]*Institute of Particle and Nuclear Physics of the Faculty of Mathematics and Physics of the Charles University, 180 00 Prague 8, Czech Republic*
[36]*University of Chicago, Chicago, IL 60637, USA*
[37]*Chung-Ang University, Seoul 06974, South Korea*
[38]*CIEMAT, Centro de Investigaciones Energéticas, Medioambientales y Tecnológicas, E-28040 Madrid, Spain*
[39]*University of Cincinnati, Cincinnati, OH 45221, USA*
[40]*Centro de Investigación y de Estudios Avanzados del Instituto Politécnico Nacional (Cinvestav), Mexico City, Mexico*
[41]*Universidad de Colima, Colima, Mexico*
[42]*University of Colorado Boulder, Boulder, CO 80309, USA*
[43]*Colorado State University, Fort Collins, CO 80523, USA*
[44]*Columbia University, New York, NY 10027, USA*
[45]*Comisión Nacional de Investigación y Desarrollo Aeroespacial, Lima, Peru*
[46]*Centro de Tecnologia da Informacao Renato Archer, Amarais - Campinas, SP - CEP 13069-901*
[47]*Central University of South Bihar, Gaya, 824236, India*
[48]*Institute of Physics, Czech Academy of Sciences, 182 00 Prague 8, Czech Republic*
[49]*Czech Technical University, 115 19 Prague 1, Czech Republic*
[50]*Dakota State University, Madison, SD 57042, USA*
[51]*University of Dallas, Irving, TX 75062-4736, USA*
[52]*Laboratoire d'Annecy de Physique des Particules, Univ. Grenoble Alpes, Univ. Savoie Mont Blanc, CNRS, LAPP-IN2P3, 74000 Annecy, France*
[53]*Daresbury Laboratory, Cheshire WA4 4AD, United Kingdom*
[54]*Dordt University, 700 7th St NE, Sioux Center, IA 51250, USA*
[55]*Drexel University, Philadelphia, PA 19104, USA*
[56]*Duke University, Durham, NC 27708, USA*
[57]*Durham University, Durham DH1 3LE, United Kingdom*
[58]*University of Edinburgh, Edinburgh EH8 9YL, United Kingdom*
[59]*Universidad EIA, Envigado, Antioquia, Colombia*
[60]*Eötvös Loránd University, 1053 Budapest, Hungary*
[61]*ETH Zurich, Zurich, Switzerland*
[62]*Faculdade de Ciências da Universidade de Lisboa - FCUL, 1749-016 Lisboa, Portugal*
[63]*Universidade Federal de Alfenas, Poços de Caldas - MG, 37715-400, Brazil*

[64]*Universidade Federal de Goias, Goiania, GO 74690-900, Brazil*
[65]*Universidade Federal do ABC, Santo André - SP, 09210-580, Brazil*
[66]*Universidade Federal do Rio de Janeiro, Rio de Janeiro - RJ, 21941-901, Brazil*
[67]*Fermi National Accelerator Laboratory, Batavia, IL 60510, USA*
[68]*University of Ferrara, Ferrara, Italy*
[69]*University of Florida, Gainesville, FL 32611-8440, USA*
[70]*Florida State University, Tallahassee, FL, USA*
[71]*Fluminense Federal University, 9 Icaraí Niterói - RJ, 24220-900, Brazil*
[72]*Università degli Studi di Genova, Genova, Italy*
[73]*Georgian Technical University, Tbilisi, Georgia*
[74]*University of Granada & CAFPE, 18002 Granada, Spain*
[75]*Gran Sasso Science Institute, L'Aquila, Italy*
[76]*Laboratori Nazionali del Gran Sasso, L'Aquila AQ, Italy*
[77]*University Grenoble Alpes, CNRS, Grenoble INP, LPSC-IN2P3, 38000 Grenoble, France*
[78]*Universidad de Guanajuato, Guanajuato, C.P. 37000, Mexico*
[79]*Harish-Chandra Research Institute, Jhunsi, Allahabad 211 019, India*
[80]*Harvard University, Cambridge, MA 02138, USA*
[81]*University of Hawaii, Honolulu, HI 96822, USA*
[82]*University of Houston, Houston, TX 77204, USA*
[83]*University of Hyderabad, Gachibowli, Hyderabad - 500 046, India*
[84]*Idaho State University, Pocatello, ID 83209, USA*
[85]*Institut de Física d'Altes Energies (IFAE)—Barcelona Institute of Science and Technology (BIST), Barcelona, Spain*
[86]*Instituto de Física Corpuscular, CSIC and Universitat de València, 46980 Paterna, Valencia, Spain*
[87]*Instituto Galego de Física de Altas Enerxías, University of Santiago de Compostela, 15782 Santiago de Compostela, Spain*
[88]*Illinois Institute of Technology, Chicago, IL 60616, USA*
[89]*Imperial College of Science Technology and Medicine, London SW7 2BZ, United Kingdom*
[90]*Indian Institute of Technology Guwahati, Guwahati, 781 039, India*
[91]*Indian Institute of Technology Hyderabad, Hyderabad, 502285, India*
[92]*Indiana University, Bloomington, IN 47405, USA*
[93]*Istituto Nazionale di Fisica Nucleare Sezione di Bologna, 40127 Bologna BO, Italy*
[94]*Istituto Nazionale di Fisica Nucleare Sezione di Catania, I-95123 Catania, Italy*
[95]*Istituto Nazionale di Fisica Nucleare Sezione di Ferrara, I-44122 Ferrara, Italy*
[96]*Istituto Nazionale di Fisica Nucleare Laboratori Nazionali di Frascati, Frascati, Roma, Italy*
[97]*Istituto Nazionale di Fisica Nucleare Sezione di Genova, 16146 Genova GE, Italy*
[98]*Istituto Nazionale di Fisica Nucleare Sezione di Lecce, 73100 - Lecce, Italy*
[99]*Istituto Nazionale di Fisica Nucleare Sezione di Milano Bicocca, 3 - I-20126 Milano, Italy*
[100]*Istituto Nazionale di Fisica Nucleare Sezione di Milano, 20133 Milano, Italy*
[101]*Istituto Nazionale di Fisica Nucleare Sezione di Napoli, I-80126 Napoli, Italy*
[102]*Istituto Nazionale di Fisica Nucleare Sezione di Padova, 35131 Padova, Italy*
[103]*Istituto Nazionale di Fisica Nucleare Sezione di Pavia, I-27100 Pavia, Italy*
[104]*Istituto Nazionale di Fisica Nucleare Laboratori Nazionali di Pisa, Pisa PI, Italy*
[105]*Istituto Nazionale di Fisica Nucleare Sezione di Roma, 00185 Roma RM, Italy*

[106]*Istituto Nazionale di Fisica Nucleare Laboratori Nazionali del Sud, 95123 Catania, Italy*
[107]*Universidad Nacional de Ingeniería, Lima 25, Perú*
[108]*Institute for Nuclear Research of the Russian Academy of Sciences, Moscow 117312, Russia*
[109]*University of Insubria, Via Ravasi, 2, 21100 Varese VA, Italy*
[110]*University of Iowa, Iowa City, IA 52242, USA*
[111]*Iowa State University, Ames, Iowa 50011, USA*
[112]*Institut de Physique des 2 Infinis de Lyon, 69622 Villeurbanne, France*
[113]*Institute for Research in Fundamental Sciences, Tehran, Iran*
[114]*Instituto Superior Técnico - IST, Universidade de Lisboa, Portugal*
[115]*Instituto Tecnológico de Aeronáutica, Sao Jose dos Campos, Brazil*
[116]*Iwate University, Morioka, Iwate 020-8551, Japan*
[117]*Jackson State University, Jackson, MS 39217, USA*
[118]*University of Jammu, Jammu-180006, India*
[119]*Jawaharlal Nehru University, New Delhi 110067, India*
[120]*Jeonbuk National University, Jeonrabuk-do 54896, South Korea*
[121]*Joint Institute for Nuclear Research, Dzhelepov Laboratory of Nuclear Problems 6 Joliot-Curie, Dubna, Moscow Region, 141980 RU*
[122]*University of Jyvaskyla, FI-40014, Finland*
[123]*Kansas State University, Manhattan, KS 66506, USA*
[124]*Kavli Institute for the Physics and Mathematics of the Universe, Kashiwa, Chiba 277-8583, Japan*
[125]*High Energy Accelerator Research Organization (KEK), Ibaraki, 305-0801, Japan*
[126]*Korea Institute of Science and Technology Information, Daejeon, 34141, South Korea*
[127]*K L University, Vaddeswaram, Andhra Pradesh 522502, India*
[128]*National Institute of Technology, Kure College, Hiroshima, 737-8506, Japan*
[129]*Taras Shevchenko National University of Kyiv, 01601 Kyiv, Ukraine*
[130]*Lancaster University, Lancaster LA1 4YB, United Kingdom*
[131]*Lawrence Berkeley National Laboratory, Berkeley, CA 94720, USA*
[132]*Laboratório de Instrumentação e Física Experimental de Partículas, 1649-003 Lisboa and 3004-516 Coimbra, Portugal*
[133]*University of Liverpool, L69 7ZE, Liverpool, United Kingdom*
[134]*Los Alamos National Laboratory, Los Alamos, NM 87545, USA*
[135]*Louisiana State University, Baton Rouge, LA 70803, USA*
[136]*University of Lucknow, Uttar Pradesh 226007, India*
[137]*Madrid Autonoma University and IFT UAM/CSIC, 28049 Madrid, Spain*
[138]*Johannes Gutenberg-Universität Mainz, 55122 Mainz, Germany*
[139]*University of Manchester, Manchester M13 9PL, United Kingdom*
[140]*Massachusetts Institute of Technology, Cambridge, MA 02139, USA*
[141]*Max-Planck-Institut, Munich, 80805, Germany*
[142]*University of Medellín, Medellín, 050026 Colombia*
[143]*University of Michigan, Ann Arbor, MI 48109, USA*
[144]*Michigan State University, East Lansing, MI 48824, USA*
[145]*Università del Milano-Bicocca, 20126 Milano, Italy*
[146]*Università degli Studi di Milano, I-20133 Milano, Italy*
[147]*University of Minnesota Duluth, Duluth, MN 55812, USA*

[148] *University of Minnesota Twin Cities, Minneapolis, MN 55455, USA*
[149] *University of Mississippi, University, MS 38677 USA*
[150] *Università degli Studi di Napoli Federico II , 80138 Napoli NA, Italy*
[151] *University of New Mexico, Albuquerque, NM 87131, USA*
[152] *H. Niewodniczański Institute of Nuclear Physics, Polish Academy of Sciences, Cracow, Poland*
[153] *Nikhef National Institute of Subatomic Physics, 1098 XG Amsterdam, Netherlands*
[154] *National Institute of Science Education and Research (NISER), Odisha 752050, India*
[155] *University of North Dakota, Grand Forks, ND 58202-8357, USA*
[156] *Northern Illinois University, DeKalb, IL 60115, USA*
[157] *Northwestern University, Evanston, Il 60208, USA*
[158] *University of Notre Dame, Notre Dame, IN 46556, USA*
[159] *University of Novi Sad, 21102 Novi Sad, Serbia*
[160] *Occidental College, Los Angeles, CA 90041*
[161] *Ohio State University, Columbus, OH 43210, USA*
[162] *Oregon State University, Corvallis, OR 97331, USA*
[163] *University of Oxford, Oxford, OX1 3RH, United Kingdom*
[164] *Pacific Northwest National Laboratory, Richland, WA 99352, USA*
[165] *Universtà degli Studi di Padova, I-35131 Padova, Italy*
[166] *Panjab University, Chandigarh, 160014 U.T., India*
[167] *Université Paris-Saclay, CNRS/IN2P3, IJCLab, 91405 Orsay, France*
[168] *Université Paris Cité, CNRS, Astroparticule et Cosmologie, Paris, France*
[169] *University of Parma, 43121 Parma PR, Italy*
[170] *Università degli Studi di Pavia, 27100 Pavia PV, Italy*
[171] *University of Pennsylvania, Philadelphia, PA 19104, USA*
[172] *Pennsylvania State University, University Park, PA 16802, USA*
[173] *Physical Research Laboratory, Ahmedabad 380 009, India*
[174] *Università di Pisa, I-56127 Pisa, Italy*
[175] *University of Pittsburgh, Pittsburgh, PA 15260, USA*
[176] *Pontificia Universidad Católica del Perú, Lima, Perú*
[177] *University of Puerto Rico, Mayaguez 00681, Puerto Rico, USA*
[178] *Punjab Agricultural University, Ludhiana 141004, India*
[179] *Queen Mary University of London, London E1 4NS, United Kingdom*
[180] *Radboud University, NL-6525 AJ Nijmegen, Netherlands*
[181] *University of Rochester, Rochester, NY 14627, USA*
[182] *Royal Holloway College London, TW20 0EX, United Kingdom*
[183] *Rutgers University, Piscataway, NJ, 08854, USA*
[184] *STFC Rutherford Appleton Laboratory, Didcot OX11 0QX, United Kingdom*
[185] *Università del Salento, 73100 Lecce, Italy*
[186] *San Jose State University, San José, CA 95192-0106, USA*
[187] *Sapienza University of Rome, 00185 Roma RM, Italy*
[188] *Universidad Sergio Arboleda, 11022 Bogotá, Colombia*
[189] *University of Sheffield, Sheffield S3 7RH, United Kingdom*
[190] *SLAC National Accelerator Laboratory, Menlo Park, CA 94025, USA*
[191] *University of South Carolina, Columbia, SC 29208, USA*

[192] *South Dakota School of Mines and Technology, Rapid City, SD 57701, USA*
[193] *South Dakota State University, Brookings, SD 57007, USA*
[194] *Southern Methodist University, Dallas, TX 75275, USA*
[195] *Stony Brook University, SUNY, Stony Brook, NY 11794, USA*
[196] *Sun Yat-Sen University, Guangzhou, 510275*
[197] *Sanford Underground Research Facility, Lead, SD, 57754, USA*
[198] *University of Sussex, Brighton, BN1 9RH, United Kingdom*
[199] *Syracuse University, Syracuse, NY 13244, USA*
[200] *Universidade Tecnológica Federal do Paraná, Curitiba, Brazil*
[201] *Tel Aviv University, Tel Aviv-Yafo, Israel*
[202] *Texas A&M University, College Station, Texas 77840*
[203] *Texas A&M University - Corpus Christi, Corpus Christi, TX 78412, USA*
[204] *University of Texas at Arlington, Arlington, TX 76019, USA*
[205] *University of Texas at Austin, Austin, TX 78712, USA*
[206] *University of Toronto, Toronto, Ontario M5S 1A1, Canada*
[207] *Tufts University, Medford, MA 02155, USA*
[208] *Universidade Federal de São Paulo, 09913-030, São Paulo, Brazil*
[209] *Ulsan National Institute of Science and Technology, Ulsan 689-798, South Korea*
[210] *University College London, London, WC1E 6BT, United Kingdom*
[211] *Valley City State University, Valley City, ND 58072, USA*
[212] *Variable Energy Cyclotron Centre, 700 064 West Bengal, India*
[213] *Virginia Tech, Blacksburg, VA 24060, USA*
[214] *University of Warsaw, 02-093 Warsaw, Poland*
[215] *University of Warwick, Coventry CV4 7AL, United Kingdom*
[216] *Wellesley College, Wellesley, MA 02481, USA*
[217] *Wichita State University, Wichita, KS 67260, USA*
[218] *William and Mary, Williamsburg, VA 23187, USA*
[219] *University of Wisconsin Madison, Madison, WI 53706, USA*
[220] *Yale University, New Haven, CT 06520, USA*
[221] *Yerevan Institute for Theoretical Physics and Modeling, Yerevan 0036, Armenia*
[222] *York University, Toronto M3J 1P3, Canada*

E-mail: roberto@lbl.gov

ABSTRACT: The rapid development of general-purpose computing on graphics processing units (GPGPU) is allowing the implementation of highly-parallelized Monte Carlo simulation chains for particle physics experiments. This technique is particularly suitable for the simulation of a pixelated charge readout for time projection chambers, given the large number of channels that this technology employs. Here we present the first implementation of a full microphysical simulator of a liquid argon time projection chamber (LArTPC) equipped with light readout and pixelated charge readout, developed for the DUNE Near Detector. The software is implemented with an end-to-end set of GPU-optimized algorithms. The algorithms have been written in Python and translated into CUDA kernels using Numba, a just-in-time compiler for a subset of Python and NumPy instructions. The GPU implementation achieves a speed up of four orders of magnitude compared with the equivalent CPU version. The simulation of the current induced on 10^3 pixels takes around 1 ms on the GPU, compared with approximately 10 s on the CPU. The results of the simulation are compared against data from a pixel-readout LArTPC prototype.

KEYWORDS: Computing, Time projection chambers, Simulation methods and programs

ARXIV EPRINT: 2212.09807

Contents

1 Introduction

The idea of using a liquid argon time projection chambers (LArTPC) for the detection of neutrino interactions was first proposed in 1977 [1]. The detection mechanism is the following: charged particles produced by neutrino interactions ionize the argon, leaving a trail of ionization electrons. In addition, liquid argon also produces scintillation light, which provides calorimetric information and a fast timing signal ($O(10$ ns) [2]). A fraction of the ionized electrons recombine immediately with the positive argon ions, while the remaining ones drift towards the anode side of the detector in a homogeneous electric field applied to the argon volume, which is usually $O(100$ V/cm). Impurities present in the LAr (e.g. O_2, H_2O, N_2) can attach a portion of the drifting electrons. The amount of drifting electrons declines as a function of the distance from the anode, since the electrons need to travel a longer path.

Typically, two or more arrays of sense wires are placed at the anode and assembled into planes. The drifting of negative charges in a constant electric field induces a signal on the wires. Each plane provides a two-dimensional image of the ionization: the position of the wire provides one

dimension, and the time of the arrival provides the second one, since the drift velocity of the electrons in the LAr is known and is typically $O(1\ \mathrm{m/ms})$. Using multiple wire planes can help estimate the position of the ionization in three dimensions. However, ambiguities arise when drifting electrons are isochronous or parallel to a wire orientation. Unambiguous 3D imaging of LArTPC charge signals is possible using a readout system based on a pixelated array of charged-sensitive pads, which has been demonstrated in ref. [3]. Both the typical distance between adjacent wires and the typical pixel pitch are in the order of few millimeters. The position on the anode plane of the involved pads provides two spatial dimensions, and the time of the induced signal provides the third one. This truly three-dimensional readout provides better reconstruction efficiency and purity than the 2D combined wire readout, as demonstrated in ref. [4].

Pixel readout requires the channel count used to be increased by a factor of 10 to 100 with respect to wire planes. Thus, with this increased channel count and granularity simulation burden, the transport of electrons in LAr and the signal induction on the pixel pads represent an ideal use case for highly-parallelized, concurrent simulation algorithms. The development of general-purpose computing on graphics processing units (GPGPU), which went hand in hand with the advances in the machine learning and deep learning fields, has driven the design of the current generation of supercomputers, such as Perlmutter at NERSC [5], which is a heterogeneous system with both GPU-accelerated and CPU-only nodes. Implementing highly-parallelized simulation chains allows full advantage of these new systems to be taken and enables the simulation of future pixelated LArTPCs, which would otherwise not be viable with current resources.

The US-based neutrino physics program relies on present and future experiments using LArTPC technology. The flagship experiment is the Deep Underground Neutrino Experiment (DUNE), which will consist of a high-intensity accelerator neutrino beam, measured by near and far detectors [6]. The Far Detector will consist of four 17-kiloton LArTPC modules located deep underground at the Sanford Underground Research Facility in Lead, South Dakota, located 1285 km from the beam source [7]. The Near Detector will be located at Fermilab, 574 m from the beam source, and will contain a 67 t modular LArTPC called ND-LAr [8].

There are already some software toolkits for LArTPCs [9, 10] and there has been some effort towards parallelizing the reconstruction stage [11]. However, the simulation stages have remained mostly sequential and their speed up has been recognized as a priority by the community [12].

In this document we will describe the implementation of a set of highly-parallelized algorithms, organized in a module called `larnd-sim` [13], that run on GPUs. They simulate the ionized electrons recombination and drifting towards the anode, the generation of electronics signals on the pixelated readout, and the processing of the signal by the front-end electronics.

2 Technical implementation

Recent rapid developments in the field of machine learning have stimulated the creation of several tool-kits for GPU-accelerated applications. In particular, the NVIDIA® CUDA platform [14] allows to use GPUs for general purpose computing via different programming languages. We opted for Numba [15], which generates CUDA computing kernels using a subset of native Python and NumPy code [16].

A CUDA kernel is a function that is executed N times in parallel by N CUDA threads. The threads can be organized in one-dimensional, two-dimensional, or three-dimensional *blocks*, which in turn can be organized in one-dimensional, two-dimensional, or three-dimensional *grids*. Blocks in the same grid contain the same number of threads, can run independently, and can be executed in any order, while threads in the same block can co-operate through shared memory. CUDA kernels typically store the result of the computation in a pre-allocated array passed to the kernel function. The CUDA programming model requires a careful design of the algorithm: the shape and size of the array where the result is stored must be known in advance and the threads must avoid race conditions during execution*, thus the result of the algorithm must not depend on the order of execution of the threads.

The software described in this document contains several CUDA kernel functions, separated into two logical categories: one for the charge simulation, described in section 3, and one for the light simulation, described in section 4. The functions simulate the detector response, including: (1) the recombination of the electrons with the argon ions, (2) the drifting of the electrons towards the anode, (3) the induction of electronic signals on the pixel pads and optical detectors, and (4) the electronics response of the charge and light readout systems.

The simulation of the passage of the initial particles through matter is performed using `edep-sim` [17], a wrapper around GEANT4 [18], which is independent from the `larnd-sim` package described here. The output consists of a set of short particle track segments, in the order of few millimeters, which describe the energy deposition trail of each particle. The length of the segments depends on the derivative of the stopping power dE/dx: the portion of a particle trail where the dE/dx changes abruptly will be divided in finer segments than the portion where the dE/dx is mostly constant. Thus, in a single segment, the energy deposition per unit length is assumed to be constant. This approximation is valid when the segment length is of the same order as the detector resolution – at much shorter lengths, fluctuations from the long tail of the dE/dx distribution fall outside of the applicable region of recombination models, and at much longer lengths, correlations in the dE/dx fluctuations become significant and the dE/dx width will be under-simulated. Within these broad considerations, reducing the minimum size of the segments has not shown a significant impact on the result of the charge simulation. This set S_i is stored in a bi-dimensional NumPy array containing the energy deposition and the spatial distribution of the segments:

$$S_i = (\vec{r}_s, \vec{r}_e, E)_i \,, \tag{2.1}$$

where $\vec{r}_s$ and $\vec{r}_e$ are four-dimensional vectors containing the spatial and timing coordinates of the segment start and end points, and E is the deposited energy. This array is used as input for our module. In order to minimize the memory transfer between the host and the device (in our case the GPU), we allocate the NumPy array directly on the device memory using CuPy [19], a GPU array backend that implements a subset of the NumPy interface. The output of the `larnd-sim` simulation is then saved in a HDF5 file [20]. The entire simulation workflow is shown in figure 1.

*In software, a race condition can happen when the behavior of the program depends on the relative timing of multiple threads or processes.

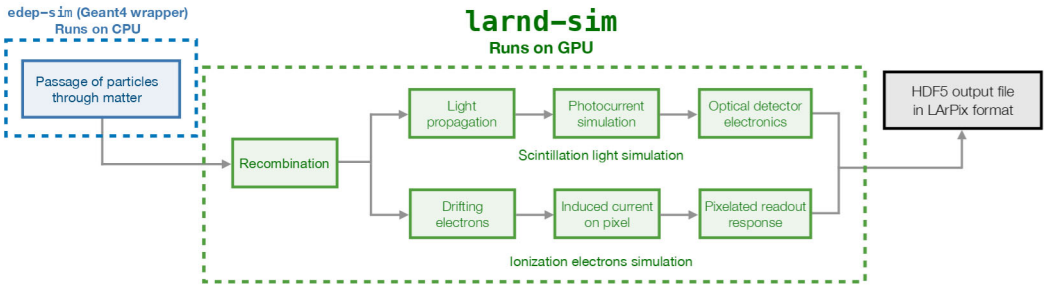

Figure 1: Diagram showing the full simulation workflow. The passage of the particle through matter is simulated by `edep-sim` on the CPU. The output is fed to `larnd-sim`, which runs entirely on GPU. Its output is finally saved in a HDF5 file.

3 Charge simulation

3.1 Electron recombination

The first step of our simulation is to calculate the number of electrons that remain after the recombination and start drifting towards the anode. We denote the initial charge ionized by the particle as Q_0, while the charge remaining after the recombination is given by $Q_R = \mathscr{R} \cdot Q_0$, where $\mathscr{R}$ is our recombination factor.

Two different models are commonly used to describe this phenomenon: the Birks model [21], which gives spurious values when applied to high-ionization particles [22], and the modified Box model [22], which doesn't suffer from these issues but is inadequate to describe particles at low stopping power (low dE/dx).

The recombination factor for the Birks model $\mathscr{R}_{\text{Birks}}$ can be parametrized as:

$$\mathscr{R}_{\text{Birks}} = \frac{A_b}{1 + k_b/\epsilon \cdot dE/dx}, \tag{3.1}$$

where A_b and k_b are free parameters that usually depend on the detector and ϵ is the product of the electric field with the liquid argon density. The ICARUS collaboration obtained $A_b = 0.800$ and $k_b = 0.0486$ (kV/MeV) (g/cm^3) [23], which are the values used in our simulation.

The recombination factor the modified Box model $\mathscr{R}_{\text{Box}}$ is defined as:

$$\mathscr{R}_{\text{Box}} = \frac{\log(\alpha + \beta/\epsilon \cdot dE/dx)}{\beta/\epsilon \cdot dE/dx}, \tag{3.2}$$

where α and β are free parameters which were measured by the ArgoNeuT collaboration to be $\alpha = 0.93$ and $\beta = 0.207$ (kV/MeV)(g/cm^3) [22]. In both cases, the typical recombination factor for a minimum ionizing particle (MIP) is around 0.7. Our simulation assumes the Birks model by default.

The implementation of the calculation of the recombination factors $\mathscr{R}_{\text{Birks}}$ or $\mathscr{R}_{\text{Box}}$ on the GPU is trivial: the i-th thread of the $K_{\text{recomb}}(S_i, \mathscr{R})$ CUDA kernel takes as input the i-th row of the NumPy array containing the segments S and applies the recombination formula, so eq. (3.1) or eq. (3.2). The result is stored in an appropriate column of the NumPy array. Currently, the simulation

treats the recombination factor as a fixed number: although this is an approximation, the level of fluctuations associated with it is significantly lower than the expected intrinsic noise of the detector, which was measured with the prototype described in section 6.

Even if this operation is computationally inexpensive, it's instructive to take a look at the performance comparison between a sequential, interpreted Python `for` loop, a loop compiled on the CPU using Numba, and the GPU implementation using a CUDA kernel. Figure 2 shows the processing time needed to calculate $\mathscr{R}_{\text{Birks}}$ of eq. (3.1) as a function of the number of GEANT4 segments given as input. The CPU-compiled version is obviously faster than the sequential interpreted loop since the function is now translated into machine code. While the CUDA kernel processing time is initially the largest, it doesn't immediately scale with the number of input segments, so it starts being the exponentially faster implementation with more than $O(10^4)$ segments, where it starts taking advantage of the massive parallelization achievable by the GPU. The NVIDIA® Tesla® V100 GPU used for this study can run more than 10^5 parallel threads. To give a figure of merit, a typical neutrino beam spill in the ND-LAr corresponds on average to $O(10^5)$ segments.

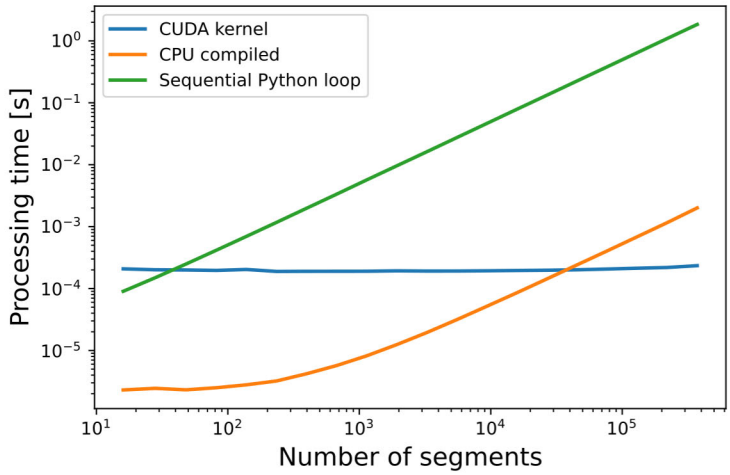

Figure 2: Processing time for the calculation of the recombination factor $\mathscr{R}_{\text{Birks}}$ of eq. (3.1) with the GPU implementation using a CUDA kernel (blue), the CPU implementation using Numba (orange), and a sequential Python `for` loop (green). For reference, a neutrino beam spill corresponds on average to $O(10^5)$ energy deposition segments in the ND-LAr. This computation was performed on a node of the NERSC Cori supercomputer, which contains two sockets of 20-core Intel Xeon Gold 6148 (Skylake) at 2.40 GHz and 8 NVIDIA® Tesla® V100 (Volta) GPUs.

3.2 Electron transport in liquid argon

The electrons remaining after the recombination travel towards the anode at a constant velocity v_{drift} (assuming perfect uniformity of the electric field), which is typically $O(1\ \text{mm}/\mu\text{s})$. The time they take to reach the anode is given by:

$$t_{\text{drift}} = (z - z_{\text{anode}})/v_{\text{drift}}, \tag{3.3}$$

where the electron drift direction is assumed to be along the z axis and where z_{anode} is the z coordinate of the anode.

The impurities in the liquid argon, such as O_2, N_2 and H_2O, can attach a portion of the drifting electrons, so electrons farther from the anode will have a higher chance to be attached. This effect is usually parametrized by a negative exponential, so the charge Q_a that effectively reaches the anode, assuming uniform impurities and a perfect electronics response, is:

$$Q_a = Q_R \cdot \exp(-t_{\text{drift}}/\tau), \tag{3.4}$$

where t_{drift} is the time the charge takes to reach the anode and τ is a parameter that depends on the concentration of impurities and it is usually called *electron lifetime*, which is in the order of milliseconds for concentrations of O_2 at tens of parts per trillion.

Electrons drifting in strong electric fields do not diffuse isotropically, so it is necessary to estimate both the longitudinal and transverse components with respect to the drift direction [24]. The diffusion length is given by:

$$\sigma = \sqrt{2Dt_{\text{drift}}}, \tag{3.5}$$

where D is the longitudinal or transverse diffusion coefficient, which depends on the electric field and liquid argon temperature. In our simulation we set the longitudinal and transverse diffusion coefficients to $D_l = 4$ cm^2/s and $D_t = 8.8$ cm^2/s, respectively. These values were obtained by a preliminary ProtoDUNE-SP [25] analysis.

This information is calculated and stored in appropriate columns of the NumPy array in a way analogous to the one described in section 3.1, where each thread processes a single segment independently.

3.3 Electronic signal induction on a pixel

3.3.1 Field response

The current induced by a point charge on a given pixel within the anode is calculated using the Shockley-Ramo theorem [26]:

$$I_{\text{pixel}} = q\ \vec{v} \cdot \nabla W, \tag{3.6}$$

where W is the *weighting field potential*, the normalized contribution of a single electrode to the overall field, q is the particle charge, and $\vec{v}$ is the velocity of the particle. Within `larnd-sim`, the induced current is pre-calculated for a point-like charge and referenced as a $I_{\text{pixel}}[t, x, y]$ look-up table (LUT). The table contains the current induced by an electron placed at discrete (x, y) locations on the anode plane at a discrete time t, where $t = 0$ is the time when the electron is at $z = 0.5$ cm. This value is chosen because of the observed flatness of the electric and weighting fields at this distance.

The $I_{\text{pixel}}[t, x, y]$ values are calculated as follows. In the region very close to the anode, the electric field and the weighting field are calculated numerically. The geometry of a small volume, including a central pixel with a pitch of 4.4 mm and its 8 nearest neighbor pixels, is modeled using CAD software and converted into a 3-dimensional mesh using the Gmsh package [27]. The fields are then calculated using the successive over-relaxation method as implemented in the Elmer FEM [28] software package. The electric and weighting fields share the same geometry, but differ in

the boundary conditions imposed on the problem. In the electric field calculation, the pixels are grounded, with the backing plane at a small offset voltage, and the field on the cathode-facing side of the volume is set to the nominal field of 500 V/cm. In the calculation of the weighting field, all electrodes other than the central pixel are grounded, the central pixel is set to unit voltage, and the voltage on the remaining conductors is set to zero. The results of these two field calculations are shown in figure 3.

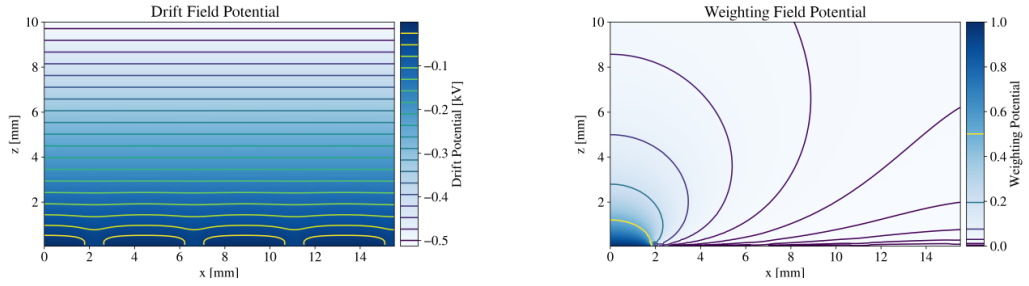

(a) Drift electric potential field in the region near the pixel plane. Shown is a slice in y along on a pixel center. The pixel surfaces are set to 0 kV, while the gradient of the far field at the surface of $z = 10$ mm is set to 0.5 kV/cm. The color scale corresponds to the value of the drift potential.

(b) Weighting potential field in the region near a "pixel of interest". The central ($x = y = 0$ pixel is set to a unit potential, while all other surfaces are set to 0 potential. The resulting unitless field defines the susceptibility to current induction by charges moving nearby.

Figure 3: The drift (left) and weighting (right) field potentials obtained by finite-element analysis in the region near a generic pixel. Shown are slices of the potential fields along an $x-z$ plane which crosses through the centerline of a pixel.

Next, the idealized drift paths (ignoring diffusion and attenuation effects) are integrated using the ICARUS and Walkowiak [29, 30] electron transport models evaluated within the calculated electric field. This model allows for the drift velocity to change as a function of the local electric field, as the assumption of a perfectly uniform field is not necessarily true very close to the anode. The drift paths are calculated for a grid of four hundred (x, y) positions, 0.5 cm from the anode on the z axis. The resulting granularity on the x and y axes is 0.33 mm. Finally, we compute the time-derivative of the weighting field potential along each path, which yields a charge-normalized current series for a given initial charge position. The sampling in time is 0.1 µs. A select few drift paths are shown in figure 4a, with their corresponding current series in figure 4b.

Farther from the pixel at $z > 0.5$ cm, the weighting potential is solved by treating the pixel as point-like and using a method-of-image-charges approximation to fix the boundary conditions at the anode and the cathode. The drift velocity is assumed to be uniform. The relative normalization to the near-field calculation is then fixed by enforcing continuity in the current series at the time boundary. Some re-scaling is performed on these current series to ensure they integrate to one electron charge, as error is introduced in the drift path integration, as well as numerical error present in the FEM solutions and their interpolated values. Figure 5 shows the tabulated induced current on a pixel up to 30 µs from the time of arrival of the drift electron. The agreement of the near-field FEM model and the dipole far-field approximation across this surface seen in figure 5

demonstrates that the transition surface at 0.5 cm is sufficiently far from the pixel plane.

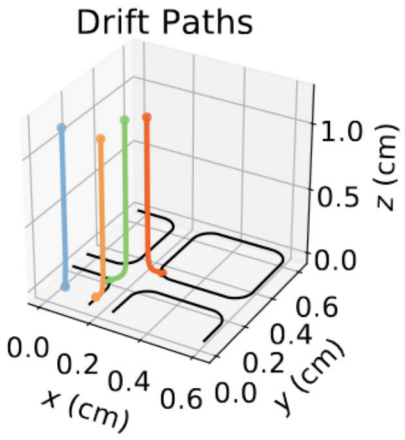

(a) Example drift paths for electrons starting at a short distance from a pixel centered at $(0, 0)$.

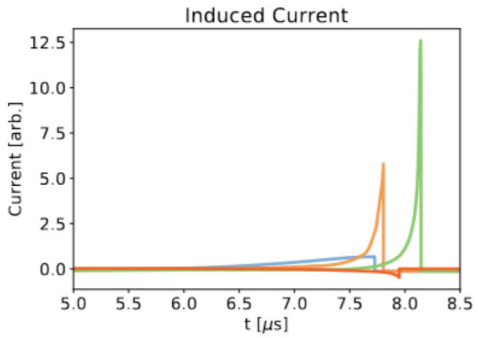

(b) Induced current on the pixel at $(0, 0)$ from example drift paths

Figure 4: To determine the near-field pixel response, we simulate the paths and velocities of drift electron within a 3D FEM field model. Here we show the simulated electron drift paths (left), and the corresponding induced current on the pixel (right) for a subset of the starting points used. The color of the trajectory on the left corresponds to the color of the current induced curve on the right.

3.3.2 Induced current calculation

The electrons drifting towards the anode are diffused in the longitudinal and transverse directions, as described in section 3.2. The ionization electrons corresponding to a GEANT4 segment will then form a three-dimensional charge cloud. The induced current on a given pixel from this can be calculated by taking the convolution of the pre-calculated pixel response model (see section 3.3.1) and the charge density of the track segment:

$$I(t) = \int I_{\text{pixel}}(t - z/v_d, x, y)\rho(x, y, z)dxdydz \tag{3.7}$$

where $\rho(x, y, z)$ is the 3-dimensional charge density including diffusion and $I_{\text{pixel}}(t - z/v_d, x, y)$ is the current response model at the given position and time tick, which is stored in the LUT described in section 3.3.1. The positively charged ions also produce a current on the pixel, however the magnitude of this current is more than 7 orders of magnitude smaller than the signal from the drift electrons due to the small drift velocity of the ions, and so it is neglected in the detector simulation.

The calculation of $I(t)$ is the most computational-intensive step of the detector simulation. In order to reduce its complexity, we apply two approximations to the charge density: first, we discretize the track segment along the track length into N points; and second, we approximate the effect of diffusion summing the contribution from M random 3D perturbations of the sample point.